Technical Paper

Journal of the Society of
Naval Architects of Korea
Vol. 25, No. 2, June 1988

Three-Dimensional Effects on Added Masses of Ship-Like Forms for Higher Harmonic Modes

by

Y.K. Chon*

Abstract

Sectional added masses of an elastic beam vibrating vertically on the free surface in higher harmonic modes are evaluated. Hydrodynamic interactions between neighboring sections, which strip theory ignors, are considered for modal wave lengths of the order of magnitude of cross-sectional dimensions of the body. An approximate solution of modified Helmholtz equation which becomes a singular perturbation problem at small wave lengths is secured to get an analytic expression for added masses attending higher harmonic modes. As a bound of the present theory, the modified Helmholtz equation is solved for the long flat plate vibrating at high frequency on the water surface without any limitations on modal frequency. Finally, extensive series of numerical calculations are carried out for ship-like forms. It is found that when modal wave length is comparable to or shorter than a typical cross-sectional dimension of a body, sectional interaction effects are large which result in considerable reductions in added masses. For a fuller section, the ratio of added mass reduction is greater. In the limit of vanishing sectional area, the added masses approach to that of flat plate of equal beam.

It is shown that the added mass distribution for a Legendre modal form can be determined from the present theory and that the results agree with the extensive three-dimensional determination of Vorus and Hilarides.

1. Introduction

In preliminary ship design, the hull is frequently considered to be a simple free-free beam. The almost universal method employed to evaluate hydrodynamic added mass for use in vibration analysis is F.M. Lewis's[1] classical procedure based on strip theory. To correct the overestimated strip theory added mass for three-dimensionality, he developed approximate correction factors, called J-factors. This procedure was developed almost simultaneously by J.L. Taylor[2]. L. Landweber and E.O. Macagno[3] extended Lewis's work for cross-sections of arbitrary shapes, vibrating in vertical and in horizontal directions. The above two-dimensional methods [1, 2, 3] still can provide fairly reliable results even in the case of higher modal frequencies. However, it has been generally recognized as being of rigor inconsistent with that attemped in the structural aspects of modern-day ship vibration analysis, which is particularly true in the case of such as propeller-induced higher mode vibration and it is difficult to guess with consistent accuracy in adv-

Manuscript received: December 5, 1987, revised manuscript received: March 7, 1988
* Member, Korean Register of Shipping

ance. This is based on the fact that hydrodynamic interaction between sections is negligible when the cross-sectional dimension of the body is small compared with modal wave length, while it is no longer valid to consider sectional added masses to be independent of neighboring sections in case of higher modes vibration.

Three-dimensional analyses[4, 5] were made by E.O. Macagno and L. Landweber. However, they are all limited for special type of body configurations and motions. The most extensive three-dimensional procedure was made by W.S. Vorus and S. Hylarides[6]. They successfully calculated longitudinal distributions of sectional added masses of a ship of arbitrary sectional shape by distributing Rankine sources on the discretized quadrilaterals on the body surface corresponding to the mode shapes represented by normalized derivatives of Legendre functions. W.C. Webster[7] has also used elaborate numerical methods to calculate the pressure distribution on the sections deforming in two- and in three-dimension.

In this study, a much less elaborate but none-the-less effective hydrodynamic theory and software are developed to evaluate the secional added masses of an elastic beam vibrating vertically in higher harmonic modes. In fact, propeller induced exciting forces are of typically 8- to 13-noded vibration[6]. Under these circumstances, the modal wave length is of the order of magnitude of cross-sectional dimension of the body, i.e., $k\bar{B}\sim O(1)$, where $\bar{B}$ denotes a typical cross-sectional dimension of the body(most usually the beam), while the strip theory rests on the assumption that $k\bar{B}\sim O(\varepsilon)$. Therefore, throughout this paper, $k\bar{B}\sim O(1)$ is assumed and mode shapes are considered to have sinusoidal variation. Numerical calculations are made for the sections of ship-like forms; circular section, elliptical sections and Lewis form sections of various parameters such as sectional area ratios, draft half-beam ratios and miner-major axis ratios. It is found that the three-dimensional effects are larger in fuller sections than in finer sections, which results in generally greater reduction ratios in added mass coefficients. Also, as modal wave length decreases, sectional area ratio effect on the added masses becomes smaller so that the added masses of the sections of equal beam-draft ratio are found to approach to the same value as that of flat plate of equal beam in an extreme case. This is verified by solving the problem of a long flat plate vibrating at high frequency on the free surface without any limitations on modal wave length. Effects of various parameters on the sectional added masses are discussed.

Finally, longitudinal distributions of ratios of three-dimensional to two-dimensional added masses, so called J-factors and hydrodynamic forces of Lewis-form Series 60 model ($\bar{B}/L=0.151$), are calculated for the eight-noded harmonic-vibration mode. Hydrodynamic force components corresponding to the eight-noded vibration of Legendre function mode shape, $\dot{P}_9$ $(2X/L)$, are extracted from the forces of harmonic eight-noded vibration mode and compared with Vorus's results[6]. The correlation is excellant between the two methods. This assures the usefulness of the present technique on the analysis of higher modes vibration.

2. Formulation

Consider a floating beam vibrating vertically in a deep, invicid, incompressible fluid. The induced motion of the fluid is assumed to be irrotational and hence a velocity potential exists. With coordinate axes as shown in Fig. 1 and assuming the cross sectional properties of the beam vary slowly longitudinally, and if furthermore, the mode shapes can be approximately considered to have sinusoidal

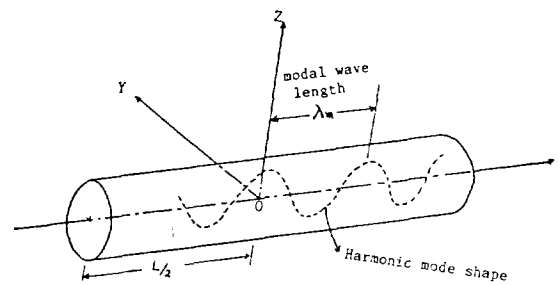

Fig. 1 Coordinate system

variation, the velocity potential $\Phi(X, Y, Z; t)$ and body velocity $V(X; t)$ at the section may be taken to be proportional to $e^{ikx} \cdot e^{i\omega t}$ without losing generality, where k is modal wave number and last term denotes the harmonic time factor which will be omitted hereafter. Then,

$$\Phi(Z, Y, Z; t) = \phi(Y, Z) e^{ikx} \cdot e^{i\omega t}$$
$$V(X; t) = V_0 e^{ikx} \cdot e^{i\omega t} \quad (1)$$

Using Eq. (1), our three-dimensional boundary value problem can be reduced to a two-dimensional one. The three-dimensional Laplace equation is converted to a modified Helmholtz equation in cross flow variables, Y and Z. Corresponding equations are

$$(\nabla^2_{Y,Z} - k^2)\phi = 0, \text{ everywhere in the water} \quad (2)$$

$$-\frac{\partial \phi}{\partial n} = \vec{V} \cdot \vec{n}_{2D}, \text{ on the body boundary} \quad (3)$$

$$\phi = 0, \text{ on } Z = 0 \quad (4)$$

$$\phi \text{ and } \frac{\partial \phi}{\partial Z} \to 0, \text{ as } Z \to -\infty \quad (5)$$

and a radiation condition in the far field.

Note that, although Eq. (2) is written in two-dimensional plane of cross-section of the beam, three-dimensional effects are included in terms of sectional potential $\phi(Y, Z)$ and modal wave number, k. Exact solution of Eq. (2) is limited to special cases, however one may seek to exploit the condition imposed by higher modes of vibration. It can be seen at once that if k is sufficiently small, which is for the case of lower harmonic modes, $k\bar{B} \sim O(\varepsilon)$, the term $k^2\phi$ may be neglected, so that we are led to the classical slender body or strip theory. However, imposing the inverse condition, namely, the reciprocal of the wave number is small compared with the cross-sectional dimension, $k\bar{B} \sim O(1)$, by dividing Eq. (2) through by k^2,

$$\frac{1}{k^2}\left(\frac{\partial^2 \phi}{\partial Y^2} + \frac{\partial^2 \phi}{\partial Z^2}\right) - \phi = 0 \quad (6)$$

Eq. (6) is seen to a singular perturbation problem, since $1/k^2$ multiplies the terms containing the highest derivatives, in which the outer solution is $\phi = 0$, except in a narrow region (or mathematical boundary layer)[8, 9] whose width is of order of $1/k$ about the section of the body.

Then all the activity takes place within this layer which serves as a transition zone to permit the velocity potential to vary from its value on the boundary to zero at its outer edge as described in Figs. 2.1 and 2.2. The thickness of this boundary layer is assumed to be very small in comparison with the dimensions of the body as well as the local radius of curvature of any point on the body so that it becomes permissible to consider that the shape and flow vary slowly in the local tangential direction y, but rapidly in local normal direction z, on the body section. This is an analogous argument with the method of stretching coordinates in solving the singular perturbation problem valid within the mathematical boundary layer [8, 9] as shown in Figs. 2.1 and 2.2.

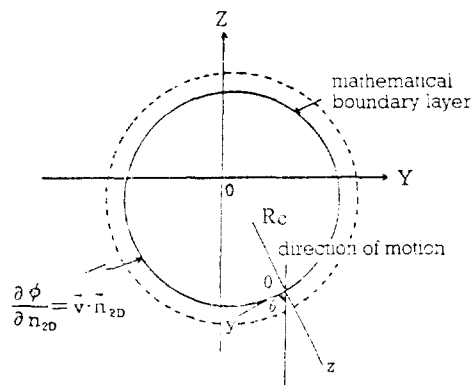

Fig. 2.1 Boundary layer description

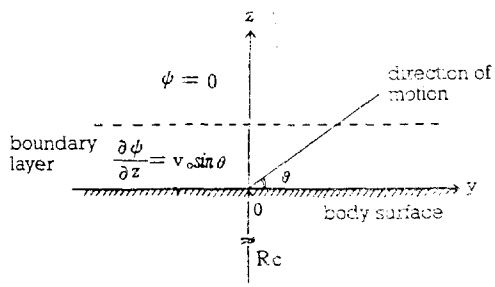

Fig. 2.2 Inner boundary value problem

3. Solution

3.1. Inner Boundary Potential

With the foreging preparations, a corresponding boundary value problem which is valid only inside of the boundary layer can be posed in terms of local coordinate system o-yz, with y axis taken in tangential direction and z axis in normal direction at the point about the section considered as described in Figs. 2.1, 2.2. Transforming the coordinate system in Eq. (2) from O-YZ to o-yz and use of the relation between local radius of curvature and

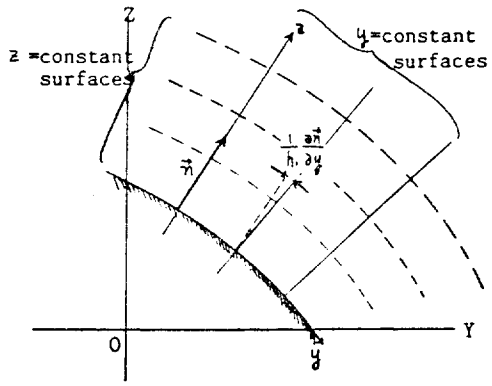

Fig. 3 Radius of curvature in transformed plane

scale factors in y and z axes [10] as shown in Fig. 3, the inner boundary-value problem corresponding to Eqs. from (2) to (5) can be written as

$$\frac{\partial^2\psi}{\partial z^2}+\frac{1}{R_c}\frac{\partial\psi}{\partial z}-k^2\psi=0,$$

in the boundary layer (7)

$$\frac{\partial\psi}{\partial z}=V_0\sin\theta, \text{ on the body surface} \quad (8)$$

$$\psi=0, \text{ outside the boundary layer} \quad (9)$$

where ψ denotes the velocity potential within the boundary layer, θ is the angle between y axis and direction of motion and local radius of curvature R_c at the point on the surface can be expressed as [10]

$$R_c=[1+(dZ+dY)^2]^{1.5}/(d^2Z/dY^2)$$

in O-YZ system (10)

or

$$R_c=\frac{1}{h_1h_2}\cdot\frac{\partial h_1}{\partial z} \text{ in } o\text{-}yz \text{ system}$$

where h_1, h_2 are the scale or metric lengths in y and z directions respectively governing coordinate transform from O-YZ to o-yz system. When R_c is infinitely large, namely, for flat surface, the contribution of the normal velocity on the surface inside of the boundary layer can be neglected, so that Eq. (7) can be reduced to

$$\partial^2\psi/\partial z^2-k^2\psi=0, \quad |R_c|\to\infty \quad (11)$$

Although Eq. (11) is not the real case, the results of application of this equation on the circular section is quite accurate as shown in Fig. 5. This assures the validity of the assumption that when the thickness of boundary layer is sufficiently small compared with local radius of curvature, which means large k, the potential within the boundary layer can be regarded as a function of only the normal direction on the surface of the section.

When R_c is finite, the velocity potential inside of the boundary layer at any point about the section is

$$\psi(z)=-\frac{V_0}{k_0}\sin\theta\cdot e^{-k_0z}, \quad |R_c| \text{ finite} \quad (12)$$

where

$$k_0=(1\pm\sqrt{1+(2kR_c)^2})/2R_c, \quad R_c\gtrless 0$$

while the solution of Eq. (11) with the same boundary condition is,

$$\psi(z)=-\frac{V_0}{k}\sin\theta\cdot e^{-kz}, \quad |R_c|\to\infty \quad (13)$$

The linearized hydrodynamic pressure on the surface about the section can be calculated from unsteady Bernoulli equation. With the omission of detailed procedure,

$$p\Big]_{z=0}=-\rho\frac{\partial\psi}{\partial t}\Big]_{z=0}=i\omega\rho\frac{V_0}{k_0}\sin\theta$$

Therefore, the linearized hydrodynamic force in the direction of motion per unit circumferential length is

$$\frac{\partial F}{\partial S}=p\Big]_{z=0}\cdot\vec{k}\cdot d\vec{S}=i\omega\rho\frac{V_0}{k_0}\sin^2\theta dS \quad (14)$$

Then, the expression of the force for total section at longitudinal position X far from the origin of the coordinate is

$$F=\oint\frac{\partial F}{\partial S}dS\cdot e^{ikx}=i\omega V_0\cdot\left\{\rho\oint\frac{\sin^2\theta}{k_0}dS\right\}$$
$$e^{ikx}=i\omega V_0\cdot M\cdot e^{ikx} \quad (15)$$

where $\oint$ donotes the integration about the circum-

ference below the waterline. Since $i\omega V_0$ is the acceleration due to velocity V_0, M can be interpreted as a sec- tional added mass per unit acceleration. Corresponding expression to Eq.(13) can be given as

$$M=\rho \oint \frac{\sin^2\theta}{k} dS, \quad |R_c| \to \infty \tag{16}$$

On the other hand, the exact solution of Eqs. (2) to (5) is available for the circular section, i.e., by the method of separation of variables in polar coordinates, it can be seen that

$$\phi(r,\theta)=\frac{V_0 \sin\theta}{kK_1'(kR)} \cdot K_1(kr) \tag{17}$$

where r and θ denote the radial and tangential directions in polar coordinates, K_1 and K_1', are the modified Bessel functiton of the second kind and its derivative with respect to argument respectively. Then the hydrodynamic force and added mass can be written as

$$F=-i\omega\rho \cdot V_0 \oint \frac{K_1(kR)}{kK_1'(kR)} \sin^2\theta \, dS \cdot e^{ikx}$$

$$M=-\frac{\rho\pi R}{2} \cdot \frac{K_1(kR)}{kK_1'(kR)} \tag{18}$$

Eq. (17) is valid for all k and therefore subsumes strip theory. As $k \to 0$, Eq. (18) yields the well-known two-dimensional result as can be deduced from the small argument behavior of K_1 and K_1'. When k approaches infinity, employing the asymptotic expansion of Bessel function for large argument in Eq. (18) yields

$$M=\frac{1}{2} \cdot \frac{\rho\pi R}{k} \tag{19}$$

3.2. Added Masses of Lewis Forms and Elliptical Sections

Applications are made of the present technique to Lewis forms and elliptical sections. As in Ref.[1], generation of Lewis form section can be done by the transformation of unit circle in $U(\xi,\eta)$ plane to $W(Y,Z)$ plane by following parametric equations.

$$U(\xi,\eta)=\xi+i\eta \tag{20}$$
$$W(Y,Z)=Y+iZ=U+A_1U^{-1}+A_3U^{-3}$$

Then

$$Y=(1+A_1)\cos\alpha+A_3\cos(3\alpha)$$
$$Z=(1-A_1)\sin\alpha-A_3\cos(3\alpha) \tag{21}$$

For given sectional area ratio σ and draft half-beam ratio H, parametric constants A_1 and A_3 can be determined. On the other hand, the equation of ellipses with semiminor and major axes being D and B are given as

$$Z=-D\sqrt{1-(Y/B)^2} \tag{22}$$

with their area ratio $\sigma=\pi/4$ and draft half-beam length ratio $H=D/B$. With foregoing preparations, all factors in the integration in Eq.(13) can be expressed in terms of parameters α, H, σ and coordinate axes Y and Z.

4. Added Mass of a Long Flat Plate at High Frequency on the Free Surface

As with the same argument from Eq.(2) to Eq. (5), let $\Phi(X,Y,Z;t)=\phi(Y,Z)e^{ikx} \cdot e^{i\omega t}$, following boundary value problem can be written, as depicted in Fig. 4,

$$(\nabla^2_{Y,Z}-k^2)\phi=0 \text{ everywhere in the water} \tag{23}$$

$$\frac{\partial\phi}{\partial Z}=V_0, \text{ for } |Y|<B, \text{ all } X \tag{24}$$

$$\phi=0 \text{ for } |Y|\geq B, \text{ all } X \tag{25}$$

Also the radiation condition in the far field must be satisfied.

4.1. Singular Integral Equation

Fundamental solution of Eq.(23) with the condition for outgoing waves in the far field is,

$$G_s(Y,Z;\gamma,\zeta)=K_0(kr)$$
$$=K_0(k\sqrt{(Y-\gamma)^2+(Z-\zeta)^2}) \tag{26}$$

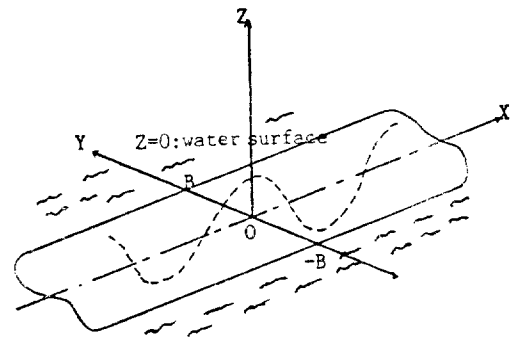

Fig. 4 Vibration of a long flat plate on the water surface

where K_0 is the modified Bessel function of the second kind of order zero, G_s can be interpreted as the velocity potential at (Y, Z) due to a quasi source of unit strength located at (η, ζ). By differentiating Eq.(26) with respect to dummy variable ζ, a potential of vertical dipole on the plate which has the property needed in this problem can be obtained as [11]

$$G_d(Y, Z; \eta, \zeta) = -\frac{\partial G_s}{\partial \zeta}\Big]_{\zeta=0} = \frac{-kZ \cdot K_1(k\sqrt{(Y-\eta)^2+Z^2})}{\sqrt{(Y-\eta)^2+Z^2}} \tag{27}$$

It can be easily seen that the limiting values of this potential on and below the plate, when $Z \to \pm 0$, differ by the amount equal to the doublet strength. i.e.,

$\phi(Y, 0^-) - \phi(Y, 0^+) = \mu(Y)$

Therefore, distribution of this dipole of strength $\mu(Y)$ along Y axis ($\zeta=0$) leads to resulting total potential

$$\phi(Y, Z) = -\frac{kZ}{2\pi}\int_{-B}^{B} \frac{\mu(\eta) \cdot K_1(k\sqrt{(Y-\eta)^2+(Z-\zeta)^2})}{\sqrt{(Y-\eta)^2+Z^2}} d\eta \tag{28}$$

Letting $\phi_0(Y, 0^-) = \mu(Y)/2$ and applying the boundary condition Eq.(24) yield,

$$\frac{\partial \phi}{\partial Z}_{Z=0} = -\frac{k}{\pi}\int_{-B}^{B} \frac{\phi_0(\eta)\ K_1(k|Y-\eta|)}{|Y-\eta|} d\eta = V_0 \tag{29}$$

This equation is seen to be a singular integral equation due to the behavior of the kernel in the integrand at $\eta = Y$. Furthermore, the kernel in Eq.(29) exhibits quadratic singular behavior at $\eta = Y$ due to the behavior of K_1 at $\eta = Y$. To isolate this singularity, addition and subtraction of the singular term in Eq.(29) yields

$$-\frac{k}{\pi}\int_{-B}^{B} \frac{\phi_0(\eta)}{k(Y-\eta)^2} d\eta = V_0 - \frac{k}{\pi}\int_{-B}^{B}\left\{\frac{1}{k(Y-\eta)^2} - \frac{K_1(k|Y-\eta|)}{|Y-\eta|}\right\}\phi_0(\eta) d\eta \tag{30}$$

Integrating Eq.(30) by parts and utilizing the condition given by Eq.(25) yields[12, 13]

$$-\frac{1}{\pi}\int_{-B}^{B} \frac{\partial \phi_0(\eta)}{\partial \eta} \frac{d\eta}{(Y-\eta)} = V_0 - \frac{k}{\pi}\int_{-B}^{B}\left\{\frac{1}{k(Y-\eta)^2} - \frac{K_1(k|Y-\eta|)}{|Y-\eta|}\right\}\phi_0(\eta) d\eta \tag{31}$$

Now the kernel on the right hand side of Eq.(31) is not singular at $\eta = Y$, while Cauchy principal-value integral appears in left hand side. Eq.(31) is of the form of a Fredholm integral equation of the second kind. It is to be solved numerically; a successive approximation method is employed in the present calculation to get the solution. It is to be noted that the integral term on the right side of Eq.(31) represents the three-dimensional or "k-effect" on $\mu(Y)$, hence in two-dimensional case, there is no contribution from this integral term, whereas increasing contribution is indicated as k becomes larger.

4.2. Numerical Solution

To solve Eq.(31), care must be taken because of the kernel on the right side of Eq.(31). Although this kernel is regular in the entire range of k, $|Y| < B$ and $|\eta| < B$, the value of this kernel does not behave uniformly since $k|Y-\eta|$ and $|Y-\eta|$ vary independently which appear in the nominator and denominator of the kernel. This non-uniformity produces a non-convergence of the solution when using the method of successive approximation. To overcome these numerical difficulties, non-dimensionalized quantities are introduced as $Y' = Yk$, $\eta' = \eta k$ in Eq.(31) and then it becomes

$$-\frac{k}{\pi}\int_{-kB}^{kB} \frac{\partial \phi_0(\eta'/k)}{\partial \eta'} \cdot \frac{d\eta'}{(Y'-\eta')} = V_0 - \frac{k}{\pi}\int_{-kB}^{kB}\left\{\frac{1}{(Y'-\eta')^2} - \frac{K_1(|Y'-\eta'|)}{|Y'-\eta'|}\right\}\phi_0(\eta'/k) d\eta' \tag{32}$$

Now the second term in the integral of right hand side of Eq.(32) behaves uniformly with $|Y'-\eta'|$, while the integral limits are changed to $\pm kB$.

The solution for Eq.(32) can be represented implicitly as, by the method of successive approximation[14],

$$\frac{k}{\pi}\int_{-kB}^{kB} \frac{\partial \phi_0^{(m)}(\eta'/k)}{\partial \eta'} \cdot \frac{d\eta'}{(Y'-\eta')} = V^{(m)}(Y'),\quad V^{(0)}(Y') = V_0,\quad (m \geq 0,\ \text{integer})$$

with

$$V^{(m+1)}(Y')=V_0-\frac{k}{\pi}\int_{-kB}^{kB}\left\{\frac{1}{(Y'-\eta')^2}-\frac{K_1(|Y'-\eta'|)}{|Y'-\eta'|}\right\}\phi_0^{(m)}(\eta'/k)d\eta'$$

and

$$\phi_0^{(m)}=(kB)\sum_{n=1}^{m}\frac{a_n}{n}\sin(n\theta);\ \lim_{m\to\infty}\phi_0^{(m)}=\phi_0(Y,0)$$

Once the potential distribution on the plate is dertermined, it is straightforward to secure the added mass, i.e., sectional hydrodynamic force can be written as

$$F=-i\omega\rho\int_{-B}^{B}\phi_0(Y)dY=i\omega V_0\cdot\left\{-\frac{\rho}{V_0}\int_{-B}^{B}\phi_0(Y)dY\right\} \tag{33}$$

5. Longitudinal Distribution of Sectional Added Masses and Hydrodynamic Forces

Applications of the present technique are made to obtain a longitudinal distribution of so called J-factors and hydrodynamic forces for 8-noded harmonic vibration. In Ref.[6], a Series-60 hull form was used by Vorus et. al., in their analyses, in which the sections were replaced by Lewis form of equal draft-half beam and area ratio and fore-aft symmetry was imposed to save computer time. J-factors and hydrodynamic forces are calculated for the same hull and the spheroid of equal B/L in the present analyses.

Introducing a dimensionless coordinate $\tilde{X}$ such that $\tilde{X}=2X/L$ and wave number $\tilde{k}$, as $\tilde{k}=kL/2$, where X is the longitudinal coordinate with its origin at the midship as dipicted in Fig. 1, and L is the total length of the hull,

then

$$|\tilde{X}|=|2X/L|\leqq 1,\ \text{for}\ |X|\leqq(L/2),\ kX=\tilde{k}\tilde{X} \tag{34}$$

Therefore, the modal function of harmonic vibration with even numbers of node can be written as

$$H(\tilde{X})=\cos\tilde{k}\tilde{X}=\cos\frac{(m-1)\pi}{2}\cdot\tilde{X} \tag{35}$$

with m defined as odd integer ($m\geqq 1$), so that $m=1$ denotes heave mode vibration. $m=3$ denotes 2 node vibration. And from Eq.(34),

$$\tilde{k}\tilde{X}=\frac{\pi}{2}(m-1)\tilde{X}=\frac{(m-1)\pi}{L}X=kX,\ kB=\left(\frac{B}{L}\right)(m-1)\pi \tag{36}$$

5.1. J-Factors

Lewis[1] first defined J-factors as the ratio of the fluid kinetic energy due to the spheroid vibrating with specified one dimensional mode shape to the fluid kinetic energy of the same spheroid by strip theory. These are called spheroid J-factors by Vorus et. al.[6] and they calculated Series 60 J-factors as the ratio of three- to two-dimensional sectional added masses. Their mode shapes are assumed to be the normalized derivatives of Legendre functions which is defined as in [15].

$$\dot{P}_m(\tilde{X})/\sqrt{m(m+1)},\ m\geqq 1 \tag{37}$$

where m being same definition as above. In fact, the coefficient in Eq.(37) arises from the normalization process [15]. In the present analysis, harmonic modal functions in terms of cosine function are used. Then J-factors corresponding to this mode shape can be calculated as in the same way in Ref. [6]

$$J_m^H(\tilde{X})=M_m^H(\tilde{X})/M_{2D}(\tilde{X}) \tag{38}$$

where $M_m^H(\tilde{X})$ and $M_{2D}(\tilde{X})$ denote sectional added mass for higher harmonic mode with $(m-1)$ nodes and strip-theory added mass respectively. In Eq. (38), two-dimensional added mass data are taken from the results of Landweber's[3].

As seen in Fig. 10.1, the spheroid J-factors are constant for all $\tilde{X}$ since the cross sections are circles.

Series 60 J-factors are found larger than those of the speroid in harmonic mode, while, as can be seen in Ref.[6], they oscillate about and are generally larger than those of the spheroid in Legendre mode shape.

5.2. Hydrodynamic Forces

Hydrodynamic force distribution is calculated to relieve the concern over the large differences in J-factors between Series 60 and the spheroid. Nondimensionalized hydrodynamic force for harmonic mode shape with $(m-1)$ nodes can be written as, following the dimensionless quantity in Ref.[6]

$$\frac{F_m^H(\tilde{X})}{\rho\omega^2 B_m{}^2\chi}=\frac{M_{2D}(\tilde{X})}{\rho B_m{}^2}\cdot J_m^H(\tilde{X})\cdot\cos\frac{(m-1)}{2}\pi\tilde{X}=\frac{M_m^H(\tilde{X})}{\frac{\pi}{2}\rho B^2(\tilde{X})}\cdot\frac{\pi}{2}\left(\frac{B(\tilde{X})}{B_m}\right)^2\cdot\cos\frac{1}{2}(m-1)\pi\tilde{X} \tag{39}$$

where $F_m^H(\tilde{X})$, $J_m^H(\tilde{X})$ are hydrodynamic force and J-factor at position X for harmonic mode shape with $(m-1)$ nodes, $B(\tilde{X})$, B_m denote sectional and maximum half beam respectively, and χ denotes the amplitude of vertical motion. Through the orthogonal analysis of harmonic modal function $\cos[(m-1)\pi\tilde{x}/2]$ using normalized Legendre functions, it can be easily seen that the harmonic mode shape with specified node numbers is actually the combination of infinitely many Legendre mode shapes with every number of nodes as shown in Eq. (40).

$$\sum_{m=1}^{\infty}\left\{\frac{1}{m(m+1)}\int_{-1}^{1}\dot{P}_m(\tilde{X})\cos\frac{(m-1)\pi}{2}\tilde{X}d\tilde{X}\right\}\cdot\dot{P}_m(\tilde{X}),\quad m;\ \text{odd integer} \tag{40}$$

Thus from Eq. (39), hydrodynamic forces for the $(m-1)$-noded Legendre mode shape can be written as

$$\frac{F_m^L(\tilde{X})}{\rho\omega^2 B_2^m\chi}=\frac{M_m^H(\tilde{X})}{\frac{\pi}{2}\rho B^2(\tilde{X})}\cdot\frac{\pi}{2}\left(\frac{B(\tilde{X})}{B_m}\right)^2\cdot\left\{\frac{1}{m(m+1)}\int_{-1}^{1}\dot{P}_m(\tilde{X})\cdot\cos\frac{(m-1)\pi}{2}\tilde{X}\right\}\cdot\dot{P}_m(\tilde{X}) \tag{41}$$

while corresponding expression in Ref.[6] reads

$$\frac{F_m^L(\tilde{X})}{\rho\omega^2 B_m{}^2\chi}=\frac{M_m^L(\tilde{X})}{\rho\cdot\frac{\pi}{2}B^2(\tilde{X})}\cdot\frac{\pi}{2}\left(\frac{B(\tilde{X})}{B_m}\right)^2\cdot\dot{P}_m(\tilde{X}) \tag{42}$$

where $M_m^L(\tilde{X})$ is the sectional added mass for Legendre mode shape with $(m-1)$ nodes. Equating Eqs. (41) and (42) yields

$$M_m^L(\tilde{X})=M_m^H(\tilde{X})\cdot\left\{\frac{1}{m(m+1)}\int_{-1}^{1}\dot{P}_m(\tilde{X})\cos\frac{(m-1)\pi}{2}\tilde{X}d\tilde{X}\right\} \tag{43}$$

In Fig. 10.2, the results of Eqs. (39), (41) are shown when $m=9$ together with Vorus's results Eq. (42) from Ref.[6]. As expected, hydrodynamic forces near the stern are vanishingly small so that the differences in J-factors in the stern portion of the hull seem to be inconsequent. Hydrodynamic forces for the harmonic mode shape are found to be larger than for the Legendre mode shape. And the correlations between the results of Eq. (41) and Eq. (42) are found to be excellant. This supports the usefulness of the present technique demonstrating that it gives good results even at the extremities of ship forms. Also as seen in Eq. (43), added mass of the sections corresponding to $(m-1)$ noded Legendre mode can be evaluated from that of the harmonic mode shape of same nodes.

6. Numerical Calculation and Conclusion

Modified Helmholtz equation which becomes singular perturbation problem at small wave length is solved approximately to evaluate the sectional added masses and to investigate three-dimensional effects on these added masses for an elastic beam of ship-like sections vibrating vertically in higher harmonic modes. It is also solved exactly for the circular section and a flat plate without any limitations on modal wave number, k, as given by Eqs. (18), (33) and shown in Fig. 5. It is found that correlation between the values from present theory and the exact solution is good for entire range of k in case of circular section. When $kB=\pi$, the difference

between the results by present method and the exact solution is only 2%. However, present theory fails to provide reliable results when kB is small, as this violates our basic tanet.

With the confirmations provided by those exact solutions, extensive numerical calculations are carried out for the sections of Lewis form and ellipses as shown in Figs. from 5 to 10 using the procedure developed herein. Analyses of these results and a comparison with three-dimensional results by Vorus et al.[6] confirm that this technique and the results herein can be used practically for vibration analyses in higher modes, while they are not reliable when the modal wave length is larger than the order of magnitude of the typical crosssectional dimension. For any given sectional configurations, those can be transformed to Lewis form sections of equal sectional properties and hydrodynamic added mass

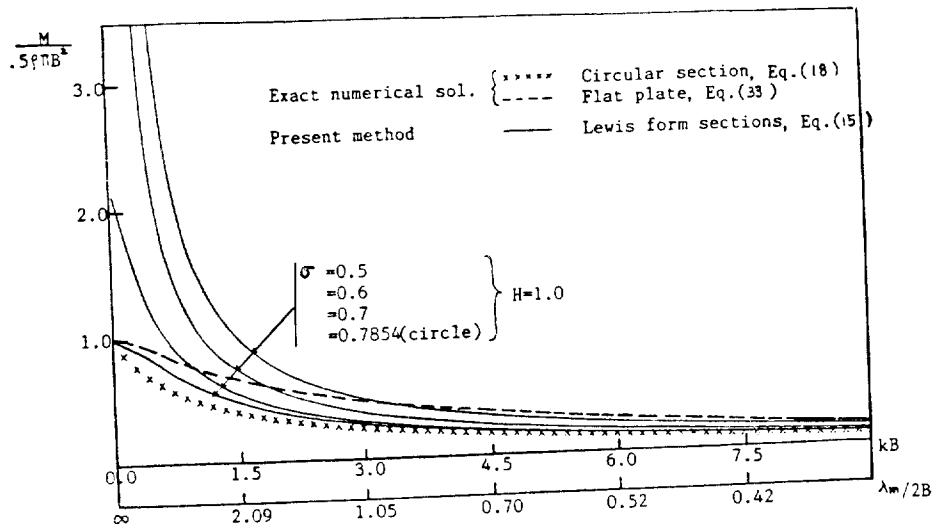

Fig. 5 M'' for flat plate, circular and Lewis form sections

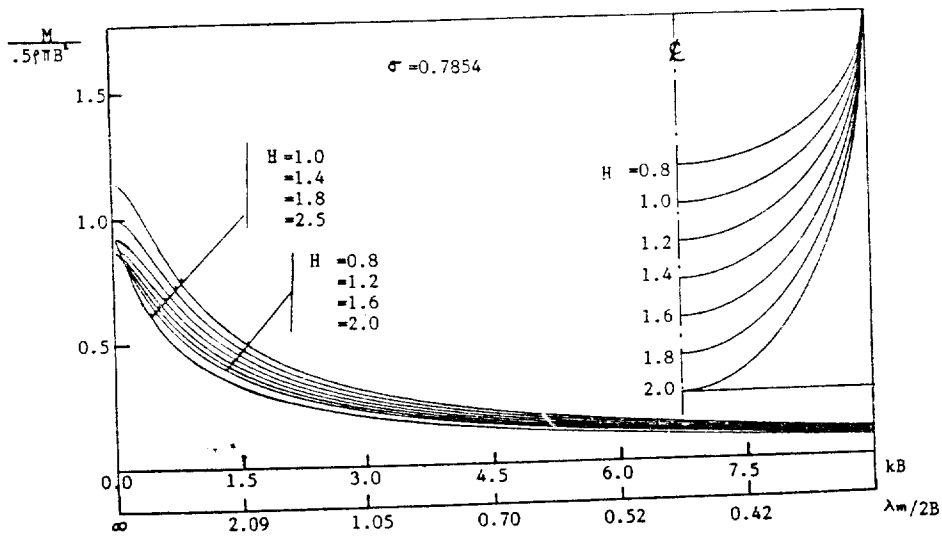

Fig. 6 M'' for elliptical sections, $H=0.8-2.5$

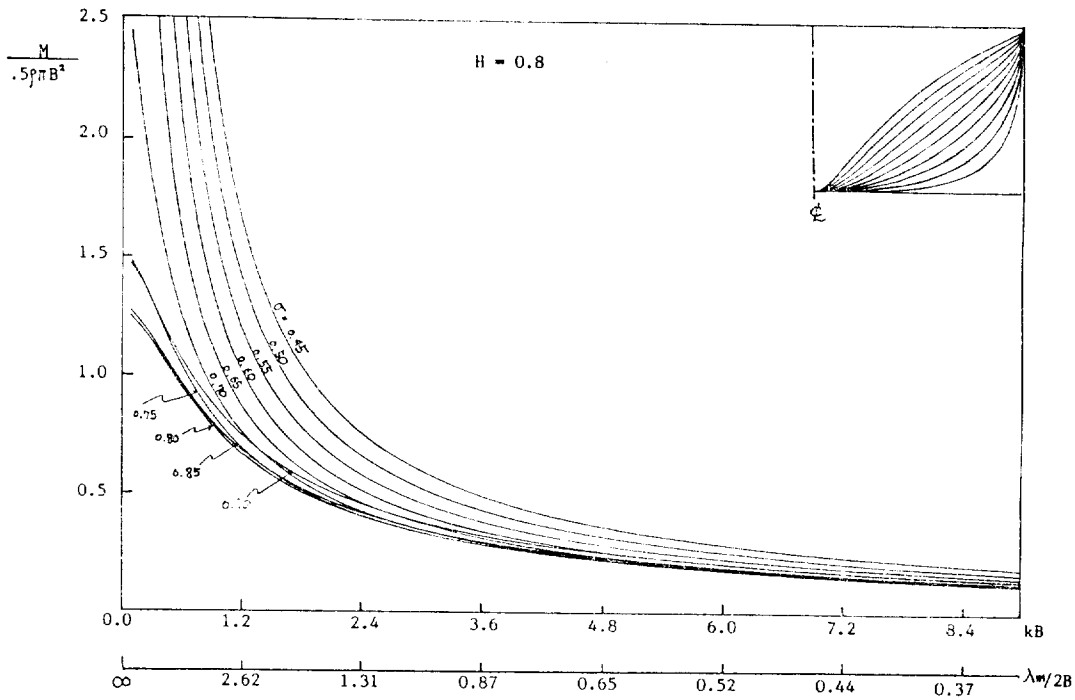

Fig. 7 M'' of Lewis form sections, $H=0.8, \sigma=0.45-0.90$

matrix under any higher modal form in the vibration analysis can be evaluated using present technique. From the foregoing discussions, following conclus ions are drawn about the higher modes added masses;

1) In Fig. 7, for Lewis form sections of equal draft half-beam ratio, H, sectional added masses decrease monotonically as modal wave number k increase. This tendency is weaker as area ratio, σ increases and H increases. Also, for equal H section, added masses of finer Lewis form sections are larger than those of fuller sections at higher modes and the differences between them become smaller for increasing k. Therefore the influence of σ on the added masses becomes smaller and finally it can be expected that the added masses of sections of finite area ratio approach to that of the flat plate of equal beam length as $k=(2\pi/\lambda_m)\to\infty$, which is shown in Fig. 5.

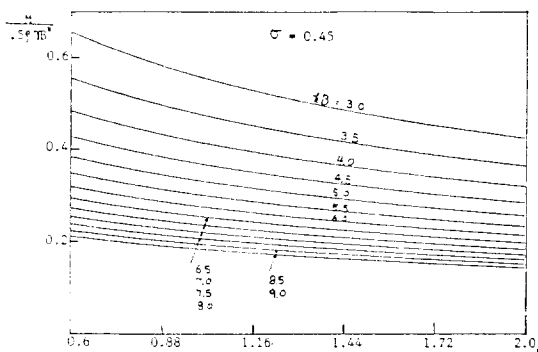

Fig. 8 M'' of Lewis forms sections, $\sigma=0.45$, $kB=3.0\sim9.0$

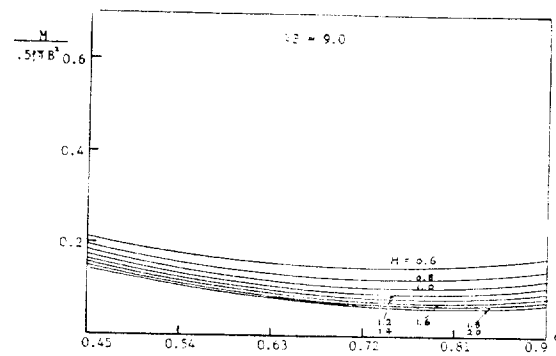

Fig. 9 M'' of Lewis form sections, $kB=9.0$, $H=0.6\sim2.0$

2) For equal area or constant σ-sections, as shown in Fig. 6 for elliptical section and Fig. 8 for Lewis form, their added masses at higher modes decrease with increasing k and H. This tendency is strong, when H is small and k is large.

3) For specific k value in higher modes as shown in Fig. 9, added mass decreases with σ until $\sigma=0.75\sim0.8$ and then increases with σ larger than about $0.75\sim0.8$.

The following conclusions can also be drawn about the three-dimensional effects on added masses. It follows that,

4) The results in the above conclusion (1) implies that the three-demensional effect along with increasing k is larger in fuller sections than for finer sections, which yields larger amount of reductions in added masses of fuller sections than those of finer sections.

5) The rate of increase of this three-dimensionality as a function of increasing σ reduces as k and H increases.

6) With the same argument as above, three-dimensional effects are stronger in larger H section for constant σ and k, and this tendency decreases with increasing σ and k.

Finally, the longitudinal distributions of J-factors and hydrodynamic force distributions are calculated for harmonic mode shape. It is found that,

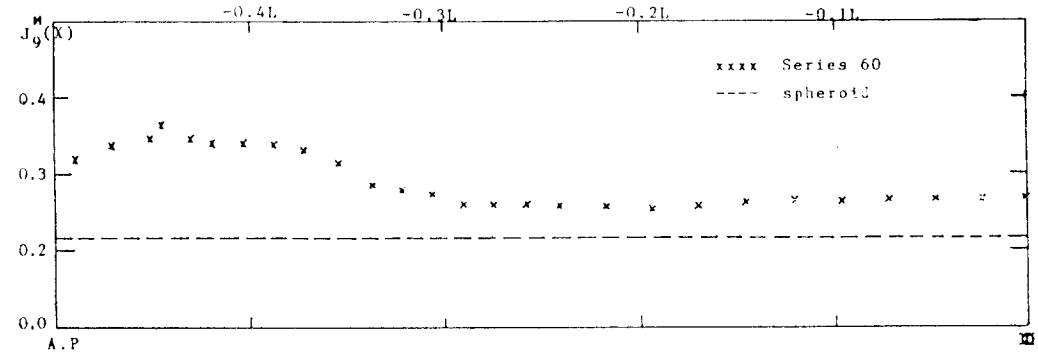

Fig. 10.1 Longitudinal distribution of J-factors of series 60 and the spheroid for eight-noded harmonic vibration

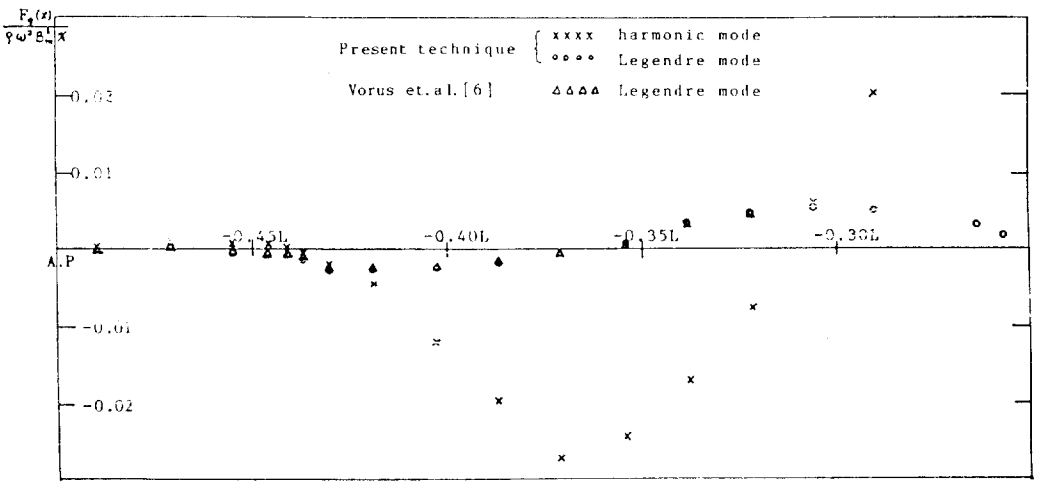

Fig. 10.2 Longitudinal distribution of hydrodynamic forces of series 60 for eight-noded harmonic vibration

7) J-factors of Series 60 are larger than those of the spheroid of equal B/L ratio for higher harmonic mode as shown in Fig. 10.1.

8) Hydrodynamic forces and added masses for higher Legendre-function type modes can be calculated from the results of harmonic mode shapes with equal nodal points through orthogonal analyses. Application of this technique shows good correlation as shown in Fig. 10.2.

References

[1] Lewis, F.M., "The Inertia of Water Surrounding a Vibrating Ship", *Trans. SNAME*, vol. 37, 1929.

[2] Tayor, J.L., "Some Hydrodynamical Inertia Coefficients", Philosophical Magazine, series 7, vol. 9, 1930.

[3] Landweber, L. and Macagno, E.O., "Added Mass of Two-Dimensional Forms Oscillating in a Free Surface", *Journal of Ship Research*, vol. 1, No. 3, 1957.

[4] Macagno, E.O. and Landweber, L., "Irrotational Motion of the Liquid Surrounding a Vibrating Ellipsoid of Revolution", *Journal of Ship Research*, Vol. 2, 1958.

[5] Landweber, L. and Macagno, E.O., "Added Mass of a Rigid Prolate Spheroid Oscillating Horizontally in a Free Surface", *Journal of Ship Research*, vol. 3, No. 4, 1960.

[6] Vorus, W.S. and Hylarices, S., "Hydrodynamic added Mass Matrix of Vibrating Ship Based on a Distribution of Hull Sources", *Trans. SNAME*, vol. 89, 1981.

[7] Webster, W.C., "Computation of the Hydrodynamic Forces Induced by General Vibration of Cylinders", *Journal of Ship Research*, vol. 23, No. 1, 1979.

[8] Milton, Van Dyke, "Perturbation Methods in Fluid Mechanics", Parabolic Press, 1975.

[9] Nayfeh, Ali Hasan, "Perturbation Method", John Wiley & Sons, 1973.

[10] Morse, Philip M. and Feshbach, H., "Methods of Theoretical Physics", McGraw-Hill Co., 1953.

[11] Kellogg, Oliver D., "Foundations of Potential Theory", Dover Publications, Inc., 1953.

[12] Miles, J.W., "The Potential Theory of Unsteady Supersonic Flows," Cambridge University Press, 1959.

[13] Miles, J.W., "On Certain Integral Equations in Diffraction Theory", *Journal of Mathematics and Physics*, vol. 28, 1949.

[14] Hildebrand, Francis B., "Methods of Applied Mathmatics", 2nd Edition, Prentice-Hall, Inc., 1965.

[15] Hobson, E.W., "Theory of Spherical and Ellipsoidal Harmonics", Cambridge University Press, 1931.